



Full Length Article

Transcranial modulation of brain oscillatory responses: A concurrent tDCS–MEG investigation

Claire J. Hanley^{a,b,1}, Krish D. Singh^a, David J. McGonigle^{a,b,*}^a CUBRIC, School of Psychology, Cardiff University, Cardiff, UK^b School of Biosciences, Cardiff University, Cardiff, UK

ARTICLE INFO

Article history:

Received 27 May 2015

Revised 13 December 2015

Accepted 14 December 2015

Available online 17 December 2015

Keywords:

Transcranial direct current stimulation

Neuromodulation

Magnetoencephalography

Brain oscillation

GABA

NMDA

ABSTRACT

Despite the increasing use of transcranial direct current stimulation (tDCS), the physiological mechanisms underlying its effects are still largely unknown. One approach to directly investigate the effects of the neuromodulation technique on the brain is to integrate tDCS with non-invasive neuroimaging in humans. To provide new insight into the neurobiology of the method, DC stimulation (1 mA, 600 s) was applied concurrently with Magnetoencephalography (MEG), while participants engaged in a visuomotor task before, during and after a period of tDCS. Responses in the motor beta band (15–30 Hz) and visual gamma band (30–80 Hz) were localised using Synthetic Aperture Magnetometry (SAM). The resulting induced and evoked oscillatory responses were subsequently analysed. A statistically significant reduction of average power in the visual gamma band was observed for anodal compared to sham stimulation. The magnitude of motor evoked responses was also found to be significantly modulated by anodal stimulation. These results demonstrate that MEG can be used to derive inferences on the cortical mechanisms of tDCS.

© 2016 The Authors. Published by Elsevier Inc. This is an open access article under the CC BY-NC-ND license (<http://creativecommons.org/licenses/by-nc-nd/4.0/>).

Introduction

Neuroimaging studies have enhanced our understanding of the physiological mechanisms underlying the effects of tDCS on behaviour (Hunter et al., 2013). Magnetic Resonance Imaging (MRI) and Spectroscopy (MRS) have provided insights into alterations of functional connectivity and changes in neurotransmitter concentrations following stimulation (Stagg et al., 2009; Clark et al., 2011; Polanía et al., 2012; Sehmi et al., 2013; Amadi et al., 2014). However, the effects of tDCS have been proposed to be temporally-specific (Stagg and Nitsche, 2011), suggesting that the use of millisecond-resolution far-field electrophysiological methods, such as Electroencephalography (EEG) and MEG, may be particularly advantageous. To date, the majority of studies combining tDCS and EEG/MEG have not used the techniques concurrently, instead focusing on the changes that occur after the period of stimulation (Polanía et al., 2011; Venkatakrisnan et al., 2011; Jacobson et al., 2012; Neuling et al., 2012; Spitoni et al., 2013). Soekadar et al. (2013) published the first concurrent tDCS–MEG study, in which a motor paradigm was used to elicit responses in the alpha and beta bands. This work focused on the feasibility of combining the techniques and found no adverse effects of stimulation on the quality of data. Since this first study, the concept of concurrent tDCS–MEG has been promoted as a potential method

to study the underpinnings of tDCS' behavioural effects. By linking observable modulations of electrophysiological activity (such as cortical oscillations; Thut et al., 2012) to electrical stimulation, this work should help to establish increasingly refined applications of tDCS in both health (through cognitive and behavioural research) and disease (as a treatment option for neurological/psychiatric disorders).

Gamma oscillations (> 30 Hz) are an appealing target for tDCS modulation due to current theories linking their generation to the excitation/inhibition balance (Buzsáki and Wang, 2012). For example, fluctuations in gamma oscillations of hippocampal pyramidal cells in rats have recently been shown to rely upon the dynamic modulation of excitation and inhibition (Atallah and Scanziani, 2009). Accordingly, enhancement in the synchrony of pyramidal cell firing is said to be propagated by a release from inhibition exerted by inhibitory post-synaptic currents (IPSCs) on GABAergic interneurons (particularly basket cells: Hasenstaub et al., 2005; Bartos et al., 2007). This suggests that pyramidal-interneuron relations are integral to the generation of gamma oscillations (Gonzalez-Burgos and Lewis, 2008). The importance of the excitation/inhibition balance has also been supported by a pharmacological MEG study, incorporating the GABA_A agonist Diazepam (Hall et al., 2010). Gamma power was increased in the visual cortex, which was proposed to reflect enhanced efficiency of fast inhibitory processing. Furthermore, the administration of alcohol, which is thought to increase GABA_A mediated inhibition and diminish glutamatergic excitation via NMDA receptors, has been shown to increase the amplitude of responses in the gamma band within visual and motor cortex (Campbell et al., 2014).

* Corresponding author at: Cardiff University Brain Research Imaging Centre, School of Psychology, Cardiff University, Cardiff, CF10 3AT, UK.

E-mail address: McGonigleD@Cardiff.ac.uk (D.J. McGonigle).

¹ Present address: Department of Psychology, Swansea University, Swansea, UK.

Oscillations in the beta band (15–30 Hz) have been proposed to be modulated by similar mechanisms to those in the gamma band (Jensen et al., 2002; Yamawaki et al., 2008). Using a resting MEG paradigm, the administration of Diazepam increased beta power and decreased peak frequency (Jensen et al., 2005). Using a basic biophysical model, the authors concluded that the elevation in beta amplitude was driven by an enhancement in the synchrony of pyramidal cell firing, driven by increased IPSC delay times that decreased the influence of inhibition and subsequently reduced beta frequency. Additionally, the GABA Transporter 1 (GAT-1) blocker Tiagabine has been shown to influence the frequency and power of event related desynchronisation (ERD) and post movement beta rebound (PMBR) responses (Muthukumaraswamy et al., 2013a). A further study compared the effects of Zolpidem (a GABA_A agonist with similar mechanisms to benzodiazepines) on slice preparations and human participants, finding that it increased beta power in both samples (Rönnqvist et al., 2013).

This proposal of causal links between the balance of cortical excitation and inhibition and the relative power of beta and gamma oscillations, suggests that oscillatory measures are ideal targets to investigate the effects of direct current stimulation on the brain. As scalp-applied anodal tDCS has been shown to increase glutamatergic transmission (primarily through NMDA receptors) and decrease GABA mediated responses (Liebetanz et al., 2002; Nitsche et al., 2003, 2004), anodal tDCS should affect gamma and beta band responses measured in MEG. However, compared to the literature highlighting the effects of cortical polarisation on motor (Nitsche and Paulus, 2001), visual (Antal et al., 2004a) and somatosensory (Matsunaga et al., 2004) evoked potentials, few studies have directly investigated the influence of DC stimulation on induced responses. Although the limited *in vitro* evidence (Bikson et al., 2004; Reato et al., 2010, 2014) and that acquired during *in vivo* investigations of beta and gamma oscillations in humans (Antal et al., 2004b; Polanía et al., 2011; Mangia et al., 2014) suggests that modulations of these rhythms should be observed.

To further the current understanding of the mechanisms underlying the effects of DC stimulation, the present study aimed to demonstrate the influence of tDCS on beta and gamma band oscillatory activity, using a combined visuomotor task (previously used by Muthukumaraswamy et al., 2013b). Task data was recorded prior to, during and after anodal and sham stimulation. Electrode configurations were designed to target primary visual and motor cortices during separate sessions. As research investigating links between tDCS and changes in oscillatory power is in its infancy, hypotheses relating to the expected effects of tDCS were generated in accordance with relevant literature (such as the outlined pharmacological-MEG research). With regard to the gamma rhythm, based on literature stating that anodal tDCS produces a decrease in GABA_A-mediated inhibition (Stagg and Nitsche, 2011), it was predicted that anodal stimulation, compared to the sham control measure, would have the opposite effect to that found following the consumption of alcohol (known to increase the efficiency of GABA_A receptors and increase inhibition; Campbell et al., 2014). Specifically, the tDCS-induced decline in inhibition was predicted to generate short IPSC durations and sporadic pyramidal cell activity (Hasenstaub et al., 2005), which would produce a decrease in gamma power. In the beta band, it was predicted that anodal stimulation would decrease the power of the ERD response and increase that of the PMBR, again by reducing GABAergic inhibition. These hypotheses are in accordance with work by Muthukumaraswamy et al. (2013a), which demonstrated that an increase in endogenous GABA levels produced opposite effects in these measures.

Materials and methods

Subjects

16 subjects took part in the study (10 males). All were aged 23–40 years ($M = 27.50$, $SD = 4.65$), had corrected-to-normal vision

and were right-hand dominant (Edinburgh Handedness Inventory, Oldfield, 1971). Upon expressing an interest in taking part in the study, subjects were screened to determine their eligibility to take part in tDCS and MEG research. Those with any contraindications were excluded from the study. Participants gave written informed consent prior to taking part in the study and all procedures were carried out with the approval of the local ethics committee (School of Psychology, Cardiff University).

Visuomotor paradigm

Participants viewed a visual stimulus composed of a vertical, stationary, square-wave grating, presented on a mean luminance background at maximum contrast with a spatial frequency of 3 cycles/degree. The visual grating subtended 8 degrees, horizontally and vertically, and featured a green fixation dot at the centre of the stimulus. The stimulus was programmed using the MATLAB Psychophysics Toolbox (Brainard, 1997; Pelli, 1997) and was presented via a Mitsubishi Diamond Pro 2070 monitor. The size of the screen was 1024 × 768 pixels with a frame rate of 100 Hz. The monitor was positioned outside of the magnetically shielded room (MSR) and was viewed through a gap in the shield, at a distance of 2.15 m. The stimulus duration was set to 1.5–2 s and was followed by a 3 s baseline period, where only the fixation dot was presented (Fig. 1). Subjects were instructed to attend to the fixation point at all times and to perform an abduction of their right index finger upon stimulus offset. The abduction responses (duration period, 1 s) were recorded via the acquisition computer.

Subjects performed three runs of the visuomotor task during each session: before (Pre), during and after (Post) stimulation. Pre and Post-tDCS runs featured 100 trials, completed in approximately 8 min. An additional 50 trials were incorporated during tDCS to accommodate the removal of epochs contaminated by the current ramp phases (where the current was gradually increased to the desired level and subsequently reduced towards zero on termination), designed to minimise sensor disturbance. These experimental runs lasted for approximately 12 min.

MEG acquisition

Whole head MEG recordings were acquired using a CTF Omega 275 channel, radial gradiometer system, sampled at 600 Hz. Excessive sensor noise necessitated that four of the channels be switched off. The remaining 271 MEG sensors were analysed as synthetic third-order gradiometers (Vrba and Robinson, 2001). An additional 29 channels were used to facilitate noise cancellation. A transistor-transistor logic pulse (TTL) was sent to the MEG system at the start of each stimulus presentation. Subjects had three electromagnetic head coils attached to the nasion and preauricular points, which were continuously localised relative to the MEG system throughout each recording. Vertical and horizontal electroculograms (EOG) were used to record eye movements. The activity of the right first dorsal interosseous (FDI) muscle was monitored via electromyogram (EMG). The finger abductions performed during the visuomotor task were recorded by the MEG system via an optical displacement system (Muthukumaraswamy, 2010).

An anatomical image for each participant was obtained for source localisation. 3D Fast Spoiled Gradient echo (FSPGR) MRI scans were acquired prior to the study, using a 3 T General Electric HDx scanner with an eight-channel head coil. Scans were acquired in an axial orientation with 1 mm isotropic voxel resolution. For co-registration of MRI images and MEG data, the positions of the electromagnetic head coils were aligned to the nasion and preauricular points, which were identifiable landmarks on the subjects' corresponding MRI images. The brain shape of each subject was extracted using FSL's Brain Extraction Tool (BET; Smith, 2002) in order to perform subsequent time-frequency analysis on the data.

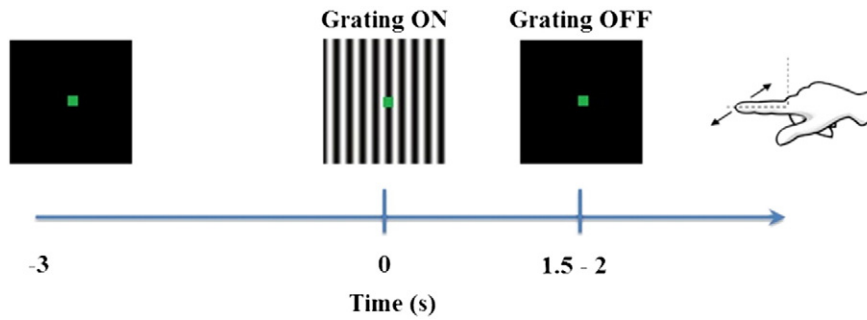


Fig. 1. A single trial of the visuomotor task. Participants attended to a stationary, square-wave grating for 1.5–2 s prior to making an abduction response with their right index finger at stimulus offset. The grating remained off for 3 s prior to each subsequent trial.

Transcranial direct current stimulation

A DC-Stimulator MR device (neuroConn, Germany) was used to deliver direct current stimulation. Subjects were randomly assigned to one of eight session orders, defined by stimulation (Anodal (A) & Sham (S)) and montage (Visual (V) & Motor (M)). The 8 session orders (of a possible 16), were not selected in accordance with a specific rationale; only such that there were orders in which each stimulation/montage type was presented at the start (first two sessions e.g. MMVV, AASS) and end (last two sessions e.g. VMMM, SSAA) of the study and also in an interleaved fashion (e.g. MVMV, ASAS). Each subject participated in 4 sessions. 3 runs of the visuomotor task (pre, during, post-tDCS) were conducted within each of these sessions. Each session took place at least 24 h apart. Both the researcher and the participant were blinded to the nature of the stimulation that took place during each session. This was made possible using the “study” mode option, in which stimulation parameters were pre-defined and executed using codes for active and sham stimulation. Stimulation duration was set to 600 s for each session, with an additional 10 s onset/offset period. Rubber electrodes, measuring 5×7 cm (35 cm^2), were attached to the scalp using conductive paste. Anodal stimulation was delivered with a current of 1 mA (current density = 0.029 mA/cm^2). For sham stimulation, the neuroConn device initially ramped up the current to mimic the peripheral effects of active tDCS before ramping down. During the stimulation period, the device continued to discharge current spikes every 550 ms ($110 \mu\text{A}$ over 15 ms) to enable continuous impedance readings. The average current over time was not more than $2 \mu\text{A}$.

Recent research has demonstrated how the effects of tDCS can extend beyond the region underneath the electrodes, thereby influencing global network dynamics (concerning both resting state and task-specific activity - Polanía et al., 2011; Amadi et al., 2014). The use of two distinct montages permitted the assessment of both local and remote modulations, allowing for such potential inferences to be made on regional specificity. For example, the modulation of visual activity could be assessed following stimulation via the alternate, motor montage and vice versa. For the visual montage (Fig. 2a), the electrodes were positioned at Oz (midline, active) and Cz (midline, reference), designed to correspond to primary visual cortex (V1) (Chatrian et al., 1985). The motor montage electrodes were situated at C3 (left hemisphere/contralateral to movement, active) and Fp2 (right hemisphere, reference), corresponding to primary motor cortex (M1; Fig. 2b).

Experimental procedure

Participants began each session by completing the consent and screening forms. Pairs of vertical and horizontal EOG electrodes were then attached around the eyes and EMG electrodes positioned over the FDI of the right hand. Three electromagnetic head coils were fitted; 1 cm above the nasion and 1 cm anterior of the preauricular points. Scalp measurements were taken to determine accurate positioning of the tDCS electrodes. After the initial preparation phase, subjects were

taken into the MSR, seated underneath the dewar in front of the computer monitor and instructed how to use the optical displacement system to perform the finger abduction responses.

Prior to the initial recording, a brief period of stimulation (~ 10 – 20 s) was delivered to determine whether impedance levels were sufficient to begin stimulation. Such durations of active stimulation have been shown to produce highly transient changes in cortical excitability, which should have returned to baseline before the onset of the first recording (Bindman et al., 1964; Purpura and McMurtry, 1965; Nitsche et al., 2003). Three runs of the task were performed per session with a brief interval (~ 5 min) between the During and Post recordings, in order for the participants to give their responses to an Adverse Effects Questionnaire (AEQ). The AEQ was administered to ascertain the presence and severity of side-effects relating to the delivery of tDCS (see Supplementary Data 1 for the questionnaire items corresponding to participant experience during stimulation). This was done in order to determine the comfort of participants’ as well as to compare their experiences of both sham and active stimulation, with regard to the efficacy of the blinding procedure. The participants stayed within the MSR during this time. Each experimental session lasted approximately 60 min.

MEG data analysis & statistics

The analysis of MEG data was performed using a variety of Linux based software, including viewer and analysis programmes from CTF (DataEditor, MRIVIEWER), in-house visualisation software (mri3dX; Krish Singh) and analysis scripts written in MATLAB (MathWorks; Cambridge, UK).

The data analysis pipeline was influenced by previous work from the MEG lab at CUBRIC. Analysis of visual and motor data was performed in a similar fashion to that outlined in a recent publication, conducted using an almost identical paradigm (Muthukumaraswamy et al., 2013b). The continuous datasets were epoched based on visual grating onset and EMG markers (-1.5 to 1.5 s visual; -1.5 to 3 s motor). The data were then visually inspected for gross artefacts and epochs were excluded from further analysis based on evidence of excessive eye blinks, muscle clenching and irregular movement displacement. Trials

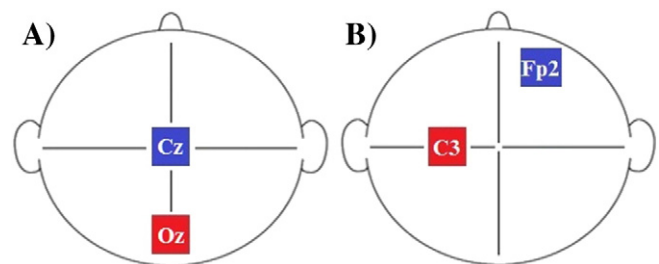


Fig. 2. Electrode configurations. Electrode positions as referenced to the 10–10 system. A) Visual stimulation montage: Oz (active), Cz (reference). B) Motor stimulation montage: C3 (active), Fp2 (reference).

corresponding to the transient current onset/offset periods during concurrent-tDCS were also discarded prior to analysis. On average, ~80% of trials were retained.

Global covariance matrices were generated in the visual gamma band (30–80 Hz) as well as motor gamma (60–90 Hz) and beta (15–30 Hz) bands. Using these covariance matrices, a set of beamformer weights were computed in a voxelwise fashion across the brain at 4 mm isotropic resolution (SAM: Robinson and Vrba, 1999; Vrba and Robinson, 2001). For source localisation, a multiple local-spheres forward model (Huang et al., 1999) was implemented. Virtual sensors were created for each beamformer voxel and Student's *t*-test images were generated to demonstrate source power changes across experimental conditions. As used by Muthukumaraswamy et al. (2013b), the following parameters were defined to determine localisation of visual gamma (−1.5 to 0 s baseline; 0 to 1.5 s active) and motor gamma (−1.3 to 1 s baseline; 0 to 0.3 s active) responses. The following parameters, adapted from Muthukumaraswamy et al. (2013a) and Campbell et al. (2014), were defined to localise motor responses in the beta band: ERD (−1.3 to −0.3 s baseline; −0.3 to 0.3 s active), PMBR (−1.3 to 0 s baseline; 1 to 2.5 s active). Tools from the FMRIB Software Library (www.fmrib.ox.ac.uk/fsl/) were used to obtain group source localisation estimates. The individual SAM images were concatenated using *fsmerge* and the mean *t*-images were generated using *fsmaths*.

The voxels demonstrating the most prominent change for each of the assessed responses were selected and virtual sensors for each individual were created for these peak regions. The data was bandpass filtered at 0.5 Hz intervals, from 1 to 100 Hz for visual responses and 1 to 120 Hz for motor responses, to assess the time–frequency response (using an 8 Hz-wide (+/− 4 Hz), third-order Butterworth filter) (Le Van Quyen et al., 2001). For each frequency interval, the Hilbert transform was used to obtain estimates of the time-varying envelope, which were then averaged across trials. Average power values were extracted from the virtual sensor data. Initially, time-frequency spectrograms were generated using non-baseline corrected, raw spectra to allow analysis of potential differences in the baseline itself. Subsequent analyses reflected changes as a percentage deviation from baseline values.

To complement the investigation of the time-varying, task-induced activity, changes in resulting evoked responses were also assessed to provide insight into modulations of timing-specific activity, locked to the onset of the visual stimulus or motor movement (Tallon-Baudry and Bertrand, 1999). This component of the study was largely exploratory as the evoked responses investigated were selected post-hoc, on the basis of their robustness. The evoked data from the corresponding virtual sensors was plotted to reflect fluctuations in the group response as a product of trial time by source amplitude. These fluctuations were classified in relation to percentage change from baseline values, having baseline-corrected the evoked data. In the motor data, an evoked response that emerged prior to movement onset and peaked shortly after was observed, followed by a post-movement reversal. The initial peak was characterised as a readiness to respond, thus reflecting the late stage of the *Bereitschaftsfield*, while the post-movement deflection signified movement execution (Deecke et al., 1982; Cheyne and Weinberg, 1989; Hallett, 2006). In accordance with previous literature, these waves are referred to as MF and MEF1, respectively (Kristeva et al., 1991). A large deflection at 100 ms was observed in the visual data (M100), corresponding to the P100 visual evoked potential and magnetic equivalent, M100 evoked field (Jeffreys and Axford, 1972a, 1972b; Brenner et al., 1975). The data from each subject was assessed to determine the greatest change in response magnitude for each of the observed waves and the latency at which it occurred. These peaks were derived by searching within a specific time window (corresponding to the start/end of the deflection). Each response was visually inspected on a subject-by-subject basis to determine the adequate range: MF (−200–200 ms), MEF1 (50–425 ms), M100 (75–150 ms).

SPSS for Windows software (Version 20; IBM, New York) was used to assess significance. As previously outlined, it was predicted that

anodal tDCS would reduce power in the gamma band. To test this hypothesis, average power values from the corresponding virtual sensor were entered into a Repeated Measures ANOVA; incorporating the factors, Time (Pre, During, Post), Montage (Visual, Motor) and tDCS (Anodal, Sham). The contribution of the between-subject factors of Montage order (VMVM, MVMV, VVMM, MMVV) and tDCS order (ASAS, SASA, AASS, SSAA) was also analysed. For the beta band, it was predicted that anodal stimulation would decrease the power of the ERD response and increase that of the PMBR. Identical analyses were used to test these hypotheses. While induced oscillatory responses are thought to be signatures of stimulus integration or “binding” and aid information transfer across local and more remote regions (Singer and Gray, 1995; Buzsáki, 2006; Donner and Siegel, 2011; Hipp et al., 2011), evoked responses have been characterised as specific to a given cortical region and associated stimulus type (Di Russo et al., 2002; Leuthold and Jentzsch, 2002). For this reason, the assessment of the influence of DC stimulation on stimulus-evoked activity was confined to that delivered via the motor montage for motor evoked responses and by the visual montage for visual evoked responses. Therefore, analysis of the peak values reflecting evoked responses did not incorporate the factor of Montage. Repeated Measures ANOVAs were also used to assess differences in impedance among the four sessions (tDCS, Montage) and to determine whether participants experienced the peripheral effects of active and sham stimulation in a similar manner; AEQ item (Tingling, Itching, Burning, Pain, Vision, Concentration, Tiredness, Unpleasant, Nervous), tDCS, Montage. Greenhouse-Geisser correction was applied where violations of sphericity were apparent. *P*-values less than 0.05 were considered significant. All *p*-values were subject to multiple comparisons correction and where a significant outcome survived this adjustment, this has been reported alongside the respective *p*-value. The correction procedure was implemented using the Benjamini-Hochberg method to control false discovery rate (FDR; Benjamini and Hochberg, 1995).

Results

Peripheral effects of tDCS

Impedance values (k Ω) were recorded at the onset of stimulation and classified by stimulation type and montage: Anodal Visual ($M = 15.41$, $SD = 0.92$), Anodal Motor ($M = 14.53$, $SD = 1.27$), Sham Visual ($M = 15.56$, $SD = 1.48$), Sham Motor ($M = 14.01$, $SD = 0.64$). No significant differences in impedance were found between tDCS stimulation types ($F(1,15) = 1.478$, $p = .243$) or their interaction with each montage (tDCS * Montage: $F(1,15) = 2.293$, $p = .151$). However, a significant main effect was established for Montage ($F(1,15) = 59.081$, $p = .000$; $p < .05$ adjusted FDR), indicating that impedance for the visual montage was higher than for the motor montage.

Analysis of ratings on the AEQ, corresponding to the period during stimulation, revealed the significant main effects of AEQ item ($F(3.073,46.099) = 8.656$, $p = .000$; $p < .05$ adjusted FDR) and tDCS ($F(1,15) = 11.575$, $p = .004$; $p < .05$ adjusted FDR). The main effect of Montage was non-significant ($F(1,15) = 2.387$, $p = .143$). The AEQ item * tDCS ($F(3.540,53.103) = 3.074$, $p = .028$) and AEQ item * Montage ($F(2.243,33.641) = 4.563$, $p = .015$) interactions were significant. Further analysis of the AEQ item * tDCS interaction found that anodal stimulation led to higher ratings than the sham condition for the items; Tingling ($t(15) = 2.828$, $p = .013$), Itching ($t(15) = 3.337$, $p = .004$; $p < .05$ adjusted FDR) and Burning ($t(15) = 2.535$, $p = .023$). In relation to the AEQ item * Montage interaction, the motor montage led to higher ratings of Itching ($t(15) = -2.702$, $p = .016$) and the visual montage led to higher ratings of tiredness ($t(15) = 2.764$, $p = .014$). Impedance and AEQ scores were largely uncorrelated. However, high Tingling ($r(16) = .606$, $p = .013$) and Itching ($r(16) = .674$, $p = .004$; $p < .05$ adjusted FDR) ratings during anodal stimulation of visual cortex were associated with high impedance values. These results indicate that participants may have been aware of the distinction between active and sham

stimulation (see Supplementary Fig. 1 for group AEQ ratings and Supplementary Data 2 for individual responses on the items experienced).

Cortical effects of tDCS

Source localisation

Consistent source localisation estimates were derived throughout the study, including those resulting from concurrent tDCS–MEG recordings (Fig. 3). Prominent bilateral occipital cortex activity was observed in the 30–80 Hz band in response to the visual grating (consistent with the literature: Swettenham et al., 2009; Muthukumaraswamy et al., 2010). Beta band motor responses (15–30 Hz) were largely confined to sensorimotor cortex of the hemisphere contralateral to the finger abduction. The ERD was situated in a posterior location (corresponding to post-central gyrus) compared to the PMBR (pre-central gyrus), as found by Jurkiewicz et al., 2006. Few subjects demonstrated consistent motor gamma responses, prohibiting the analysis of 60–90 Hz gamma band activity.

Baseline activity

Average power values corresponding to the raw, non-baseline corrected spectra were initially assessed for potential differences introduced by the neuromodulation technique. Repeated Measures ANOVAs produced no significant main effects for the analyses corresponding to the ERD (Time ($F(2,30) = 1.737, p = .193$); Montage ($F(1,15) = .679, p = .423$); tDCS ($F(1,15) = .113, p = .741$)), PMBR (Time ($F(2,30) = 1.209, p = .313$); Montage ($F(1,15) = .229, p = .639$); tDCS

($F(1,15) = 1.007, p = .331$)) or visual gamma responses (Time ($F(2,30) = .813, p = .453$); Montage ($F(1,15) = 3.329, p = .088$); tDCS ($F(1,15) = .017, p = .899$)). All associated interactions were also non-significant. The lack of significant findings in the period corresponding to the pre-stimulus baseline indicated no statistical influence of the neuromodulation technique. The stability of the pre-stimulus period, with respect to the stimulation, permitted the subsequent representation of the data in terms of relative, percentage change in the active, post-stimulus period with respect to the specified baseline period.

Task-induced responses

An average of source power was computed for the frequency bands of interest to assess modulations of the time-frequency response, using the virtual sensor data (see Appendix A for average power values).

Motor beta band response. In relation to the ERD, the factor Time marginally missed significance ($F(2,30) = 3.154, p = .057$). The main effects of Montage ($F(1,15) = .232, p = .637$), tDCS ($F(1,15) = .593, p = .453$) and all associated interactions were non-significant. For the analysis of PMBR, Time ($F(2,24) = .341, p = .715$) and tDCS ($F(1,12) = 1.104, p = .314$) were found to be non-significant. There was a significant main effect of Montage ($F(1,12) = 10.555, p = .007$; $p < .05$ adjusted FDR), coupled with a highly significant Montage * Montage order interaction ($F(3,12) = 7.673, p = .004$; $p < .05$ adjusted FDR). Further investigation determined that the motor montage resulted in higher average power changes than the visual montage, when subjects

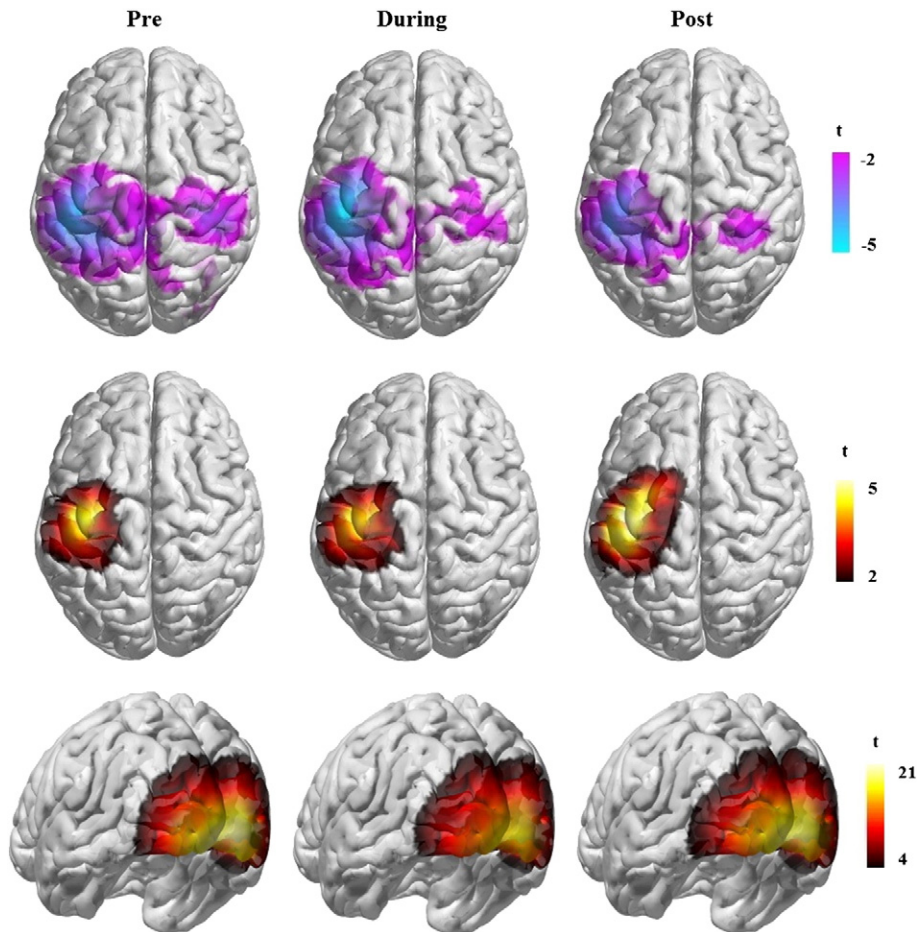


Fig. 3. Group source localisation. Results of SAM source localisation performed on each response component (top-bottom: beta-ERD, PMBR, visual gamma), across time points (left-right: Pre, During, Post-tDCS). The images show voxelwise group t-statistics, thresholded at $p < .05$ (uncorrected). These values are indicative of source amplitude changes in regions where activity significantly differed between the active and baseline period of trials. The data depicted corresponds to the experimental runs incorporating anodal stimulation, having been delivered via the visual montage for visual gamma analysis and the motor montage for the analysis of beta band activity. Results were projected onto a template brain using BrainNet Viewer (Xia et al., 2013).

performed sessions in the order MVMV ($t(3) = -9.795$, $p = .002$; $p < .05$ adjusted FDR). Fig. 4 illustrates the time-frequency response for each of the assessed intervals, within the beta band.

Visual gamma band response. Fig. 5 demonstrates the time-frequency response within the gamma band. The factor Time ($F(1.430, 17.165) = .374$, $p = .624$) was found to be non-significant. Montage ($F(1, 12) = 9.002$, $p = .011$) and tDCS ($F(1, 12) = 5.043$, $p = .044$) produced significant main effects. The Montage main effect represented a tendency for the motor montage to result in greater power changes compared to the visual montage. The main effect of tDCS corresponded to a reduction in power in the anodal compared to sham stimulation condition. All within-subject interactions were non-significant, however, there was an interaction for tDCS and the between-subject factor tDCS order ($F(3, 12) = 4.080$, $p = .033$). A trend was found for the anodal condition to produce a power reduction compared to sham stimulation, with regard to session order SSAA ($t(3) = -3.037$, $p = .056$).

Task-evoked responses

Mean latency and magnitude values for each evoked response are presented in Appendix B. The data from one participant was removed from the evoked analysis due to the absence of clearly identifiable peak responses.

Motor evoked response. The MF and MEF1 responses are illustrated in Figs. 6a and b, which demonstrate the mean evoked virtual sensor response at the source locations, in motor cortex, identified as having the greatest change in ERD and PMBR, respectively (also see Supplementary Fig. 2).

Beginning with the analysis of magnitude changes, the MF resulting from the ERD virtual sensor location produced the significant main effect of Time ($F(1.133, 15.864) = 11.654$, $p = .003$; $p < .05$ adjusted FDR). The main effect of tDCS ($F(1, 14) = 3.726$, $p = .074$) failed to reach significance. The associated interaction was, however, found to be significant (Time * tDCS: $F(1.026, 14.368) = 5.554$, $p = .032$). Greater deflections in amplitude were observed for the anodal compared to sham condition during stimulation ($t(14) = 2.346$, $p = .034$) and during anodal tDCS as opposed to pre- ($t(14) = -3.032$, $p = .009$) or post-stimulation ($t(14) = 2.888$, $p = .012$). Fig. 4b shows the time-frequency representation of the magnitude change, which corresponds to the burst of activity around 5–12 Hz observed at the time of the ERD. The MF resulting from the PMBR data failed to achieve significance with respect to the main effect of Time ($F(1.110, 15.547) = 4.089$, $p = .057$), tDCS ($F(1, 14) = 1.375$, $p = .261$) and the associated interaction (Time * tDCS: $F(1.078, 15.096) = 2.546$, $p = .130$). For the MEF1 resulting from the ERD data, the main effect of Time ($F(1.014, 14.192) = 13.280$, $p = .003$; $p < .05$ adjusted FDR), tDCS ($F(1, 14) = 5.439$, $p = .035$) and the associated interaction (Time * tDCS: $F(1.010, 14.145) = 5.380$, $p = .036$) all reached significance. This was due to greater deflections taking place during anodal compared to sham tDCS ($t(14) = -2.344$, $p = .034$) and during tDCS as opposed to pre- ($t(14) = 3.188$, $p = .007$; $p < .05$ adjusted FDR) or post-stimulation ($t(14) = -2.999$, $p = .010$). For the MEF1 PMBR data, the main effect of Time ($F(1.025, 14.346) = 4.479$, $p = .052$), tDCS ($F(1, 14) = 2.528$, $p = .134$) and the associated interaction (Time * tDCS: $F(1.039, 14.543) = 3.105$, $p = .098$) did not meet the criteria for significance.

With regard to the latency of evoked responses, analysis of the MF resulting from the ERD virtual sensor did not produce significance for

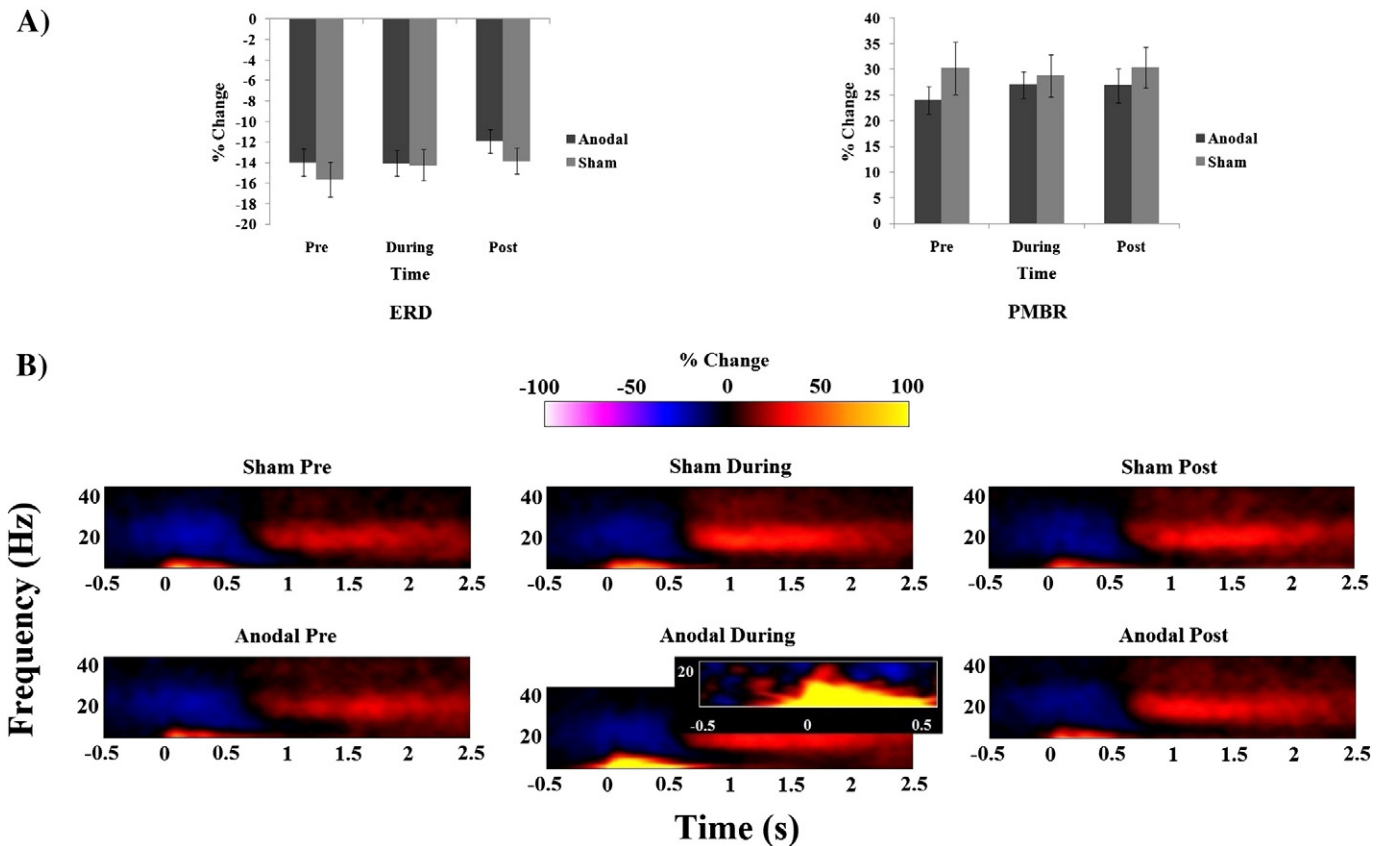


Fig. 4. Time-frequency response in the beta band. A) Mean percentage change in average power for the ERD and PMBR responses. Error bars represent ± 1 standard error (S.E.M). B) Spectrograms depict motor beta-ERD and PMBR in relation to a finger abduction response (illustrated as percentage change from baseline). Note the onset of 5–12 Hz activity in conjunction with movement onset, during anodal stimulation. The inset within the “Anodal During” panel depicts the time-frequency representation of the corresponding phase-locked component of the data. The identical pattern of movement onset activity suggests the identified 5–12 Hz response reflects an evoked as opposed to induced signal.

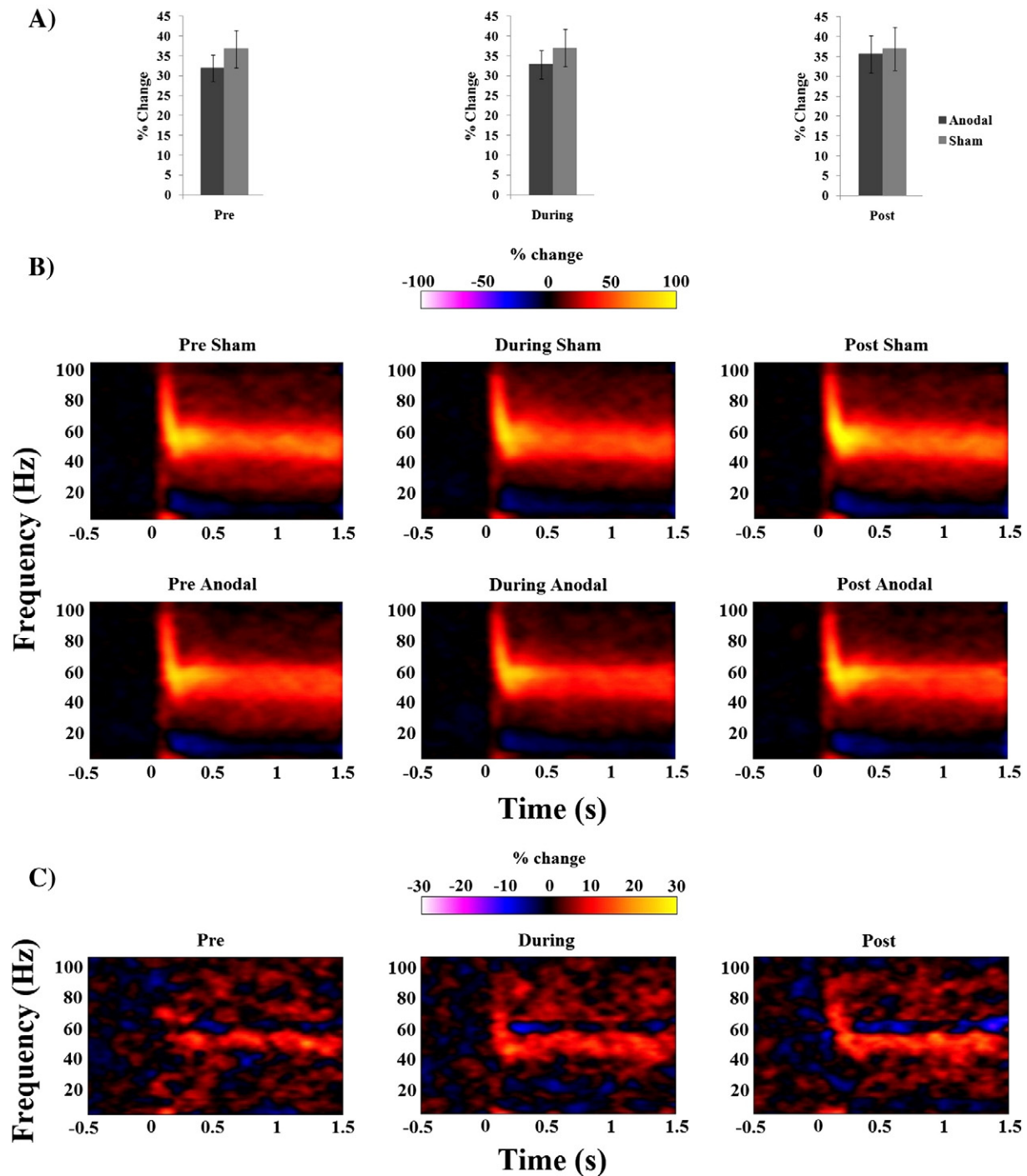


Fig. 5. Time-frequency response in the gamma band. A) Mean percentage change in average power for the visual gamma response. Error bars represent ± 1 standard error (S.E.M.). B) Spectrograms depict visual gamma band responses in relation to a stationary, square-wave grating (illustrated as percentage change from baseline). C) Difference images (Sham-Anodal) demonstrate the strength of the initial gamma 'spike' and the sustained response in the sham condition, indicating that anodal stimulation produced a reduction in power. Anodal stimulation also appears to have produced a more broadband response by elevating the sustained frequency (as illustrated by the negative amplitude change at ~60 Hz).

either main effect or the interaction (Time: $F(2,28) = 2.064$, $p = .146$; tDCS: $F(1,14) = .006$, $p = .939$; Time * tDCS: $F(2,28) = .641$, $p = .534$). The data relating to the PMBR also failed to reveal a significant main effect of Time ($F(1.489,20.845) = 2.085$, $p = .158$), tDCS ($F(1,14) = .265$, $p = .615$) or the accompanying interaction (Time * tDCS: $F(2,28) = .546$, $p = .585$). For the MEF1 resulting from the ERD, the main effect of Time ($F(2,28) = 2.943$, $p = .069$), tDCS ($F(1,14) = .530$, $p = .478$) and the associated interaction (Time * tDCS: $F(2,28) = .382$, $p = .686$) failed to reach significance. For the PMBR

data, both main effects and the interaction also failed to meet the criteria for significance (Time: $F(2,28) = 1.060$, $p = .360$; tDCS: $F(1,14) = .025$, $p = .875$; Time * tDCS: $F(2,28) = 1.228$, $p = .308$).

Visual evoked response. The M100 evoked response is illustrated in Fig. 6c, which demonstrates the mean evoked virtual sensor response at the source location, in visual cortex, identified as having the greatest change in gamma synchronisation).

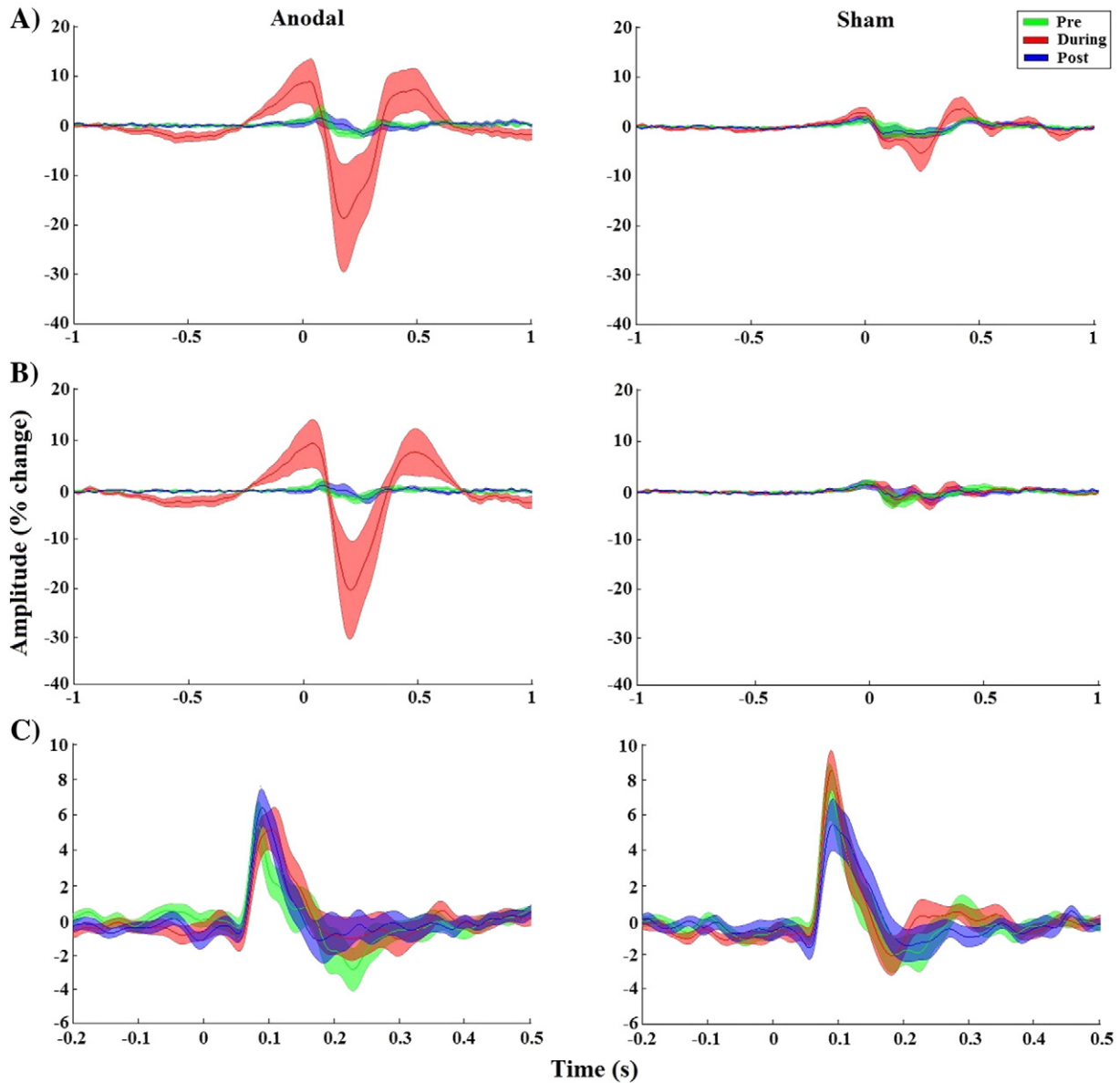


Fig. 6. Visuomotor evoked responses. Group average evoked responses for anodal (left) and sham (right) stimulation, corresponding to changes in the source amplitude of responses derived from each subject's beta-ERD (A), PMBR (B) and visual gamma (C) virtual sensor. Amplitude change is reflected as percentage change from baseline values. Line colour denotes the factor of Time and line thickness corresponds to ± 1 standard error (S.E.M.).

No within-subject main effects or the associated interaction were found to be significant for the M100 visual evoked response, with regard to magnitude (Time: $F(2,22) = 1.132$, $p = .341$; tDCS: $F(1,11) = .990$, $p = .341$; Time * tDCS: $F(2,22) = 1.304$, $p = .292$). However, the Time * tDCS order interaction was found to be significant ($F(6,22) = 2.973$, $p = .028$), whereby the significant main effect of Time ($F(1.067,3.202) = 12.801$, $p = .033$) was established for the stimulation order ASAS. Here, the magnitude of the M100 response was greater during stimulation as opposed to pre- ($t(3) = -4.739$, $p = .018$) or post-stimulation ($t(3) = 4.772$, $p = .017$) time points.

For the analysis of latency changes, the M100 response failed to produce significance for the main effects for Time ($F(2,28) = .964$, $p = .394$) and tDCS ($F(1,14) = 1.064$, $p = .320$) as well as for the associated interaction (Time * tDCS: $F(2,28) = .324$, $p = .726$).

In summary, tDCS was shown to modulate specific evoked and induced oscillatory metrics of visuomotor activity. In relation to the induced responses, average power in the visual gamma band was reduced for the anodal condition. The main effect of Montage was found to be significant during several analyses (both visual and

motor), indicating a tendency for enhanced response magnitudes when utilising the motor as opposed to visual montage. Despite the implementation of counterbalanced sessions, Montage order and tDCS order were also shown to affect electrophysiological responses. With regard to the evoked responses, the latency of the observed peaks was not significantly affected by tDCS. However, the magnitude of the MF and MEF1 waves was shown to increase during anodal stimulation (predominantly for the ERD virtual sensor location). The M100 visual response was also found to increase in magnitude during the stimulation time point, albeit in conjunction with the order in which the tDCS was presented as opposed to the stimulation itself.

Discussion

This study aimed to determine whether anodal transcranial direct current stimulation could modulate well-characterised markers of brain activity in MEG, in order to address the physiological mechanisms underpinning the neuromodulation technique. Potential modulations of both time-locked and induced responses were assessed before, during

and after stimulation. Several aspects of cortical activity were affected by the intervention. Most notably, anodal stimulation produced a reduction of average power in the visual gamma band and an increase in magnitude for the MF and MEF1 responses.

Task-induced responses

While tDCS-specific modulations were not evident for the motor responses, a significant reduction of average power in the visual gamma band was observed for the anodal condition. In accordance with the well-established physiological account of such oscillatory activity, the gamma rhythm is said to allow for insight into the status of the excitation/inhibition balance due to the underlying interplay of GABAergic interneurons and glutamatergic pyramidal cells (Bartos et al., 2007; Gonzalez-Burgos and Lewis, 2008; Buzsáki and Wang, 2012). As previously outlined, anodal tDCS is thought to perturb the balance of excitation and inhibition by reducing GABAergic neurotransmission and suppressing GABA_A receptor response, while increasing the efficiency of NMDA receptors (Creutzfeldt et al., 1962; Bindman et al., 1964; Liebetanz et al., 2002; Nitsche et al., 2003; Stagg et al., 2009; Clark et al., 2011). This physiological state is the opposite of that induced by alcohol intake, which has been shown to increase visual gamma amplitude (Campbell et al., 2014). Speculatively, by reducing the influence of GABAergic mechanisms and decreasing inhibitory tone, the release from inhibition that synchronises pyramidal cell response may have been relatively absent in the presence of anodal stimulation. This may have suppressed the likelihood of unified firing and thus produced the observed decrease in oscillatory power. Such an account explicitly supports the role of GABAergic mechanisms in the generation tDCS effects (Stagg and Nitsche, 2011). Interestingly, the reduction in average power does not appear to have been specifically associated with the visual montage (as indicated by the absence of a specific Montage * tDCS interaction), which suggests that stimulation in general, including that of motor cortex, was able to influence visual processing. The position of the cathodal electrode over Cz, close to the motor region, may have been partially responsible for this finding if visuomotor interactions were affected by a hyperpolarisation of neurons in motor cortex. However, it should be noted that the reduction in average power was found in the absence of a Time * tDCS interaction, again signifying a general outcome as opposed to a specific, temporal expression of the stimulation.

Task-evoked responses

In contrast to the induced data, only the motor evoked responses were significantly modulated by tDCS. More specifically, the magnitude of the MF and MEF1 responses was shown to be enhanced during anodal stimulation (predominantly at the site of the peak beamformer voxel from the corresponding beta-ERD analysis). Not surprisingly, the strength of the responses in question was evident in the time-frequency response, represented as a burst of 5–12 Hz activity accompanying the ERD. The functional relevance of the responses affected by the stimulation has previously been demonstrated to correspond to the preparation and subsequent execution of movement (Deecke et al., 1982; Cheyne and Weinberg, 1989; Kristeva et al., 1991; Chen et al., 1998; Chen and Hallett, 1999). Therefore, the presence of DC stimulation appears to have facilitated an increased readiness to respond and engage in task-related movement. Recently, Pellicciari et al. (2013) assessed motor cortical reactivity following tDCS, using simultaneous EEG recordings. Similar to the current study, the authors demonstrated a modulation of cortical activity with regard to anodal tDCS. Furthermore, cortical activity was closely associated with changes in corticospinal excitability. These results suggest it is likely that the observed changes in motor evoked responses were linked to alterations in corticospinal activity, which took place while the stimulation was being delivered. This places the results of the current study in accordance with the invasive neurophysiological findings that first

determined the neuronal depolarisation and elevation in spontaneous firing associated with anodal tDCS (Creutzfeldt et al., 1962; Bindman et al., 1964; Purpura and McMurtry, 1965) as well as the pioneering human studies that demonstrated the ability of anodal stimulation to increase corticospinal excitability (Nitsche & Paulus, 2000, 2001). Taken together, these results further strengthen the available evidence for the influence of anodal polarisation on motor cortex responsivity.

Comparison of modulations in induced and evoked responses

Comparing the response modulations obtained as part of the current study, the most statistically compelling effects of anodal polarisation were those related to the phase-locked, motor evoked components (indicative of basic, low-level processing of perceptual cues and subsequent movement responses; Kristeva et al., 1991). Given that tDCS modulations tend to be more pronounced in motor cortex than posterior regions (Antal et al., 2004a; Lang et al., 2007; Chaieb et al., 2008; Antal et al., 2010), the occurrence of alterations in motor responses is not surprising. The prominence of tDCS modulations during the analysis of evoked responses, as opposed to induced rhythms, can be elaborated upon in relation to the distinction between their neurobiological origins (Muthukumaraswamy et al., 2010; Cheyne, 2013). While sustained induced responses are thought to rely upon complex patterns of global and local connectivity across multiple spatial scales (related to factors that influence synchrony, such as receptor efficiency and neurotransmission), task-evoked responses are thought to arise from transient, spatially-specific changes in cortical excitability (related to the properties of a stimulus innervating a particular sensory system) (Pfurtscheller and Lopes da Silva, 1999). In this instance, it appears that tDCS did not sufficiently modulate the synaptic processes required to alter sustained oscillatory responses but did adjust local, short-lasting cortical reactivity. Accordingly, brief alterations in membrane potential have been observed during anodal polarisation of the cortex, which increase cortical excitability and spontaneous firing rate but do not induce lasting change as evidenced by the lack of after-effects (Purpura and McMurtry, 1965; Nitsche et al., 2003).

The presence of modulations only during direct current stimulation indicates that such transient alterations may have occurred in the current study. In the absence of sustained depolarisation and the resulting rise in intracellular sodium and calcium concentration, tDCS would fail to trigger a change in synaptic strength (Liebetanz et al., 2002; Nitsche et al., 2003, 2004; Fresnoza et al., 2014). In turn, GABAergic and NMDA receptor efficiency would not be modulated and the balance of excitatory and inhibitory drive thought to underlie gamma and beta oscillatory activity would remain unchanged (Bartos et al., 2007; Yamawaki et al., 2008). An absence of sufficiently consistent modulations to allow changes in synaptic plasticity to emerge may, therefore, explain the relative absence of alterations in task-induced oscillatory activity.

Methodological considerations

Transient changes in cortical excitability are often reported following short durations of DC stimulation; however, while the duration featured in the current study was comparatively extended, the length of stimulation used may have contributed to the absence of some expected findings. Certain complex cortical responses, such as those requiring neuronal synchronisation, may require extensive (longer than usual) durations of stimulation before modulations can be observed. For example, an increase in fronto-central ERD in the beta band, linked to a finger tapping task, was demonstrated after anodal stimulation of M1 but at twice the duration of the current study (20 min) (Notturmo et al., 2014). While it should be noted that local and global broadband changes in cortical synchronisation have been found following only 10 min of sensorimotor cortex stimulation, this could be attributed to the increased focality of the high-definition tDCS procedure used in this study (Roy et al., 2014).

The use of a maximum contrast stimulus may have also contributed to our findings by introducing a ‘ceiling effect’ (as previously determined by Antal et al., 2004a). To further modulate responses within a system that is already being pushed to the limit of excitation has been shown to be extremely difficult (Froc et al., 2000). Therefore, where neuronal output was likely to have been saturated by the stimulus, this may have restricted the dynamic range of any potential modulations. This would mean that the system would be unable to develop and maintain a consistently altered baseline excitation level. Stimulation would also consequently fail to modify factors, such as the rate of IPSCs on GABAergic interneurons with connections to pyramidal cells, required to alter the synchrony of oscillations (Jensen et al., 2005; Atallah and Scanziani, 2009). Consequently, change in oscillatory activity following tDCS may be more readily observed with lower contrast stimuli, and at longer stimulation durations, to give the modulation of cortical activity additional scope and time to develop.

As a potential alternative to the static polarisation delivered via tDCS, transcranial alternating current stimulation (tACS) could be used to set baseline excitability to synchronise with the dynamics of a desired frequency band. Zaehle et al. (2010) first demonstrated the influence of tACS on endogenous rhythms, showing entrainment of alpha oscillations in visual cortex. A subsequent study found that tACS at 20 Hz was able to modulate cortical responsivity in M1 and this excitability change was shown to be predicted by related changes in the beta band response (Schutter and Hortensius, 2011). A recent study has also highlighted the feasibility of concurrent tACS-EEG applications and has shown the emergence of synchronisation of alpha oscillations during 10 Hz stimulation (Helfrich et al., 2014). Simultaneous tACS-MEG also appears to be possible (as suggested by Soekadar et al., 2013 and recently implemented by Neuling et al., 2015).

A related concept to research designed to manipulate baseline excitability is that of state-dependency. Behavioural studies have highlighted the reversal or abolishment of typical tDCS effects if stimulation is delivered during task performance, particularly for tasks involving motor actions (Antal et al., 2007; Horvath et al., 2014). The current study incorporated such movement-based responses and did not record resting state MEG data, unlike a recent study that found significant modulations of oscillatory activity (Venkatakrisnan et al., 2011). Consequently, the results may be indicative of the state-dependent nature of tDCS modulations. This highlights the fragility of tDCS after-effects and suggests that their emergence may depend on the activity taking place during the stimulation period (which may largely underlie the finding of inconsistent neurophysiological modulations by tDCS; Horvath et al., 2015).

Abnormal effects of tDCS have also been demonstrated in relation to the timing of repeated stimulation. Monte-Silva et al. (2013) established that administering subsequent doses of anodal stimulation, with an inter-stimulation interval of 24 h, produced an abolishment of the expected post-stimulation elevation in motor cortex excitability. As the minimum period between sessions was 24 h in the current study, such detrimental cumulative effects may have occurred due to subsequent exposure. Additionally, it cannot be ruled out that differences in the AEQ ratings, with regard to anodal and sham stimulation, may have been related to the observed physiological responses. A comprehensive investigation of the blinding procedure was beyond the scope of the present study but assessing the experience of stimulation in this manner could represent a potentially valuable means of evaluating neural and/or behavioural outcome measures.

Finally, due to the scope of the research, a large volume of statistical tests were conducted to establish the effects of tDCS at a peripheral and cortical level. The outcome of the implemented adjustment for multiple comparisons likely reflects this as many of the results did not survive the correction applied to control false discovery rate. Future research, designed to focus on specific aspects of this initial study, would be expected to circumvent this issue.

Effects of electrode montage & stimulation order

Aside from the influence of tDCS, the electrode montage used during a given session was demonstrated to determine the nature of average power responses. This occurred in the beta and gamma bands, where the motor montage was associated with enhanced responses compared to the visual montage. This is unlikely to be due any specific aspect of the stimulation because the montages used were independent of the time points at which average power was assessed and encompassed both active and sham modalities. The greater influence of the motor montage may have been due to lower impedance values resulting from the motor montage, indicating less shunting of the current and more targeted administration to the brain.

Additionally, the reduction of average power in the visual gamma band corresponded to the order in which the tDCS was administered. This also occurred with regard to the timing of the magnitude change in the visual M100 response. This was surprising as the after-effects of tDCS, following ~10 min of stimulation, have been established to return to baseline levels within 90 min of the stimulation being terminated (Nitsche and Paulus, 2001). The wash-out interval incorporated between sessions should have also ensured that carry-over effects were unlikely to arise. These order effects were particularly unexpected in the context of the implemented counterbalancing, which should have minimised the confounding influence of stimulation order (providing that any order effects were anticipated to be linear). While persistent effects may occur following several sessions of anodal stimulation and are desirable in a clinical setting (Baker et al., 2010), specific order effects have not previously been reported where explicitly assessed (Fregni et al., 2006; Boggio et al., 2008; Mahmoudi et al., 2011). However, should these effects be genuine, it raises substantial issues concerning appropriate study design and the transience of stimulation effects.

Conclusions

Anodal tDCS was shown to modulate electrophysiological activity, primarily evoked responses. As the timing-specific modulation effects were only observed during stimulation, the results are consistent with the influence of tDCS on cortical responsivity via transient as opposed to sustained alterations in membrane potential. Accordingly, the absence of consistent changes in excitability can account for the lack of prolonged, post-stimulation changes as well as the comparative absence of change with regard to induced responses. Several factors such as stimulus contrast and the execution of motor responses during stimulation may have attenuated the typical tDCS effect. Nonetheless, the study indicates that electrophysiological metrics are likely implicated in the generation of tDCS effects. Future research will focus on establishing optimised stimulation conditions to attempt to address these issues and further investigate the underlying neurobiological mechanisms of DC stimulation.

Acknowledgments

The authors would like to thank Suresh Muthukumaraswamy (University of Auckland, NZ) for his support with regard to the core analysis pipeline and Alexander Shaw (CUBRIC) for his assistance with additional aspects of analysis and programming. The research was made possible due to the funding of the President's Research Scholarships (Cardiff University).

Conflict of interest

The authors declare that the research was conducted in the absence of any commercial or financial relationships that could be construed as a potential conflict of interest.

Appendix A

Table 1

Average power values. Mean \pm SD, calculated across the corresponding frequency band (beta: 15–30 Hz, gamma: 30–80 Hz) and reported as percentage change from baseline, pre-stimulus values.

ERD	Visual anodal	Visual sham	Motor anodal	Motor sham
Pre	-15.09 \pm 6.70	-15.94 \pm 6.19	-13.95 \pm 5.29	-15.61 \pm 6.80
During	-14.00 \pm 6.56	-13.46 \pm 6.23	-14.05 \pm 5.01	-14.21 \pm 6.15
Post	-14.06 \pm 5.15	-12.89 \pm 5.17	-11.90 \pm 4.55	-13.84 \pm 5.01
PMBR	Visual anodal	Visual sham	Motor anodal	Motor sham
Pre	26.45 \pm 15.30	26.06 \pm 17.19	24.10 \pm 10.70	30.19 \pm 20.45
During	24.41 \pm 16.09	25.40 \pm 16.68	27.00 \pm 10.12	28.83 \pm 16.45
Post	21.59 \pm 10.58	22.36 \pm 13.37	26.88 \pm 13.43	30.42 \pm 15.98
Visual gamma	Visual anodal	Visual sham	Motor anodal	Motor sham
Pre	27.51 \pm 12.28	28.33 \pm 12.15	31.96 \pm 13.34	36.71 \pm 18.96
During	25.44 \pm 11.25	28.25 \pm 12.41	32.87 \pm 14.34	36.98 \pm 18.93
Post	27.34 \pm 13.86	30.16 \pm 11.71	35.58 \pm 18.59	36.93 \pm 21.89

Appendix B

Table 1

Evoked response latency and magnitude values. Peaks were derived for each subject as the maximum or minimum value within the specified time window. Peaks from motor-based waves are reported for ERD and PMBR data. Each value represents the Mean \pm SD. Latency is given in seconds (s). Magnitude is given as percentage change from baseline values

Latency				
MF	ERD		PMBR	
	Motor anodal	Motor sham	Motor anodal	Motor sham
Pre	0.018 \pm 0.079	0.018 \pm 0.074	0.047 \pm 0.050	0.031 \pm 0.051
During	0.009 \pm 0.082	-0.002 \pm 0.087	0.030 \pm 0.059	0.027 \pm 0.081
Post	0.003 \pm 0.089	0.008 \pm 0.071	0.056 \pm 0.077	0.035 \pm 0.070
MEF1	ERD		PMBR	
	Motor anodal	Motor sham	Motor anodal	Motor sham
Pre	0.182 \pm 0.103	0.165 \pm 0.086	0.182 \pm 0.079	0.203 \pm 0.119
During	0.165 \pm 0.090	0.150 \pm 0.079	0.200 \pm 0.080	0.190 \pm 0.113
Post	0.186 \pm 0.105	0.160 \pm 0.084	0.203 \pm 0.079	0.209 \pm 0.110
M100	Visual anodal		Visual sham	
Pre		0.096 \pm 0.017		0.093 \pm 0.010
During		0.098 \pm 0.016		0.095 \pm 0.011
Post		0.098 \pm 0.012		0.093 \pm 0.011
Magnitude				
MF	ERD		PMBR	
	Motor anodal	Motor sham	Motor anodal	Motor sham
Pre	4.911 \pm 5.041	4.611 \pm 3.868	3.480 \pm 2.947	3.998 \pm 2.010
During	15.172 \pm 16.070	4.842 \pm 4.742	12.924 \pm 18.924	4.750 \pm 5.004
Post	4.712 \pm 3.952	3.668 \pm 2.685	4.563 \pm 3.929	4.833 \pm 3.826
MEF1	ERD		PMBR	
	Motor anodal	Motor sham	Motor anodal	Motor sham
Pre	-4.271 \pm 3.197	-4.687 \pm 4.048	-4.051 \pm 3.182	-5.546 \pm 4.403
During	-36.395 \pm 41.026	-10.399 \pm 12.693	-26.886 \pm 45.083	-6.941 \pm 4.789
Post	-5.234 \pm 2.470	-4.747 \pm 3.585	-4.358 \pm 3.460	-5.432 \pm 5.072
M100	Visual anodal		Visual sham	
Pre		7.944 \pm 3.520		9.376 \pm 5.786
During		7.975 \pm 4.067		9.739 \pm 4.844
Post		8.221 \pm 4.208		7.573 \pm 4.090

Appendix C. Supplementary data

Supplementary data to this article can be found online at <http://dx.doi.org/10.1016/j.neuroimage.2015.12.021>.

References

- Amadi, U., Ilie, A., Johansen-Berg, H., Stagg, C.J., 2014. Polarity-specific effects of motor transcranial direct current stimulation on fMRI resting state networks. *NeuroImage* 88, 155–161.
- Antal, A., Kincses, T.Z., Nitsche, M.A., Bartfai, O., Paulus, W., 2004a. Excitability changes induced in the human primary visual cortex by transcranial direct current stimulation: direct electrophysiological evidence. *Invest. Ophthalmol. Vis. Sci.* 45 (2), 702–707.
- Antal, A., Varga, E.T., Kincses, T.Z., Nitsche, M.A., Paulus, W., 2004b. Oscillatory brain activity and transcranial direct current stimulation in humans. *Neuroreport* 15 (8), 1307–1310.
- Antal, A., Terney, D., Poreisz, C., Paulus, W., 2007. Towards unravelling task-related modulations of neuroplastic changes induced in the human motor cortex. *Eur. J. Neurosci.* 26 (9), 2687–2691.
- Antal, A., Terney, D., Kühnl, S., Paulus, W., 2010. Anodal transcranial direct current stimulation of the motor cortex ameliorates chronic pain and reduces short intracortical inhibition. *J. Pain Symptom Manag.* 39 (5), 890–903.
- Atallah, B.V., Scanziani, M., 2009. Instantaneous modulation of gamma oscillation frequency by balancing excitation with inhibition. *Neuron* 62 (4), 566–577.
- Baker, J.M., Rorden, C., Fridriksson, J., 2010. Using transcranial direct-current stimulation to treat stroke patients with aphasia. *Stroke* 41 (6), 1229–1236.
- Bartos, M., Vida, I., Jonas, P., 2007. Synaptic mechanisms of synchronized gamma oscillations in inhibitory interneuron networks. *Nat. Rev. Neurosci.* 8 (1), 45–56.
- Benjamini, Y., Hochberg, Y., 1995. Controlling the false discovery rate: a practical and powerful approach to multiple testing. *J. R. Stat. Soc. Ser. B Methodol.* 57, 289–300.
- Bikson, M., Inoue, M., Akiyama, H., Deans, J.K., Fox, J.E., Miyakawa, H., Jefferys, J.G., 2004. Effects of uniform extracellular DC electric fields on excitability in rat hippocampal slices in vitro. *J. Physiol.* 557 (1), 175–190.
- Bindman, L.J., Lippold, O.C.J., Redfern, J.W.T., 1964. The action of brief polarizing currents on the cerebral cortex of the rat (1) during current flow and (2) in the production of long-lasting after-effects. *J. Physiol.* 172 (3), 369–382.
- Boggio, P.S., Zaghi, S., Lopes, M., Fregni, F., 2008. Modulatory effects of anodal transcranial direct current stimulation on perception and pain thresholds in healthy volunteers. *Eur. J. Neurol.* 15 (10), 1124–1130.
- Brainard, D.H., 1997. The psychophysics toolbox. *Spat. Vis.* 10, 433–436.
- Brenner, D., Williamson, S.J., Kaufman, L., 1975. Visually evoked magnetic fields of the human brain. *Science* 190, 480–482.
- Buzsáki, G., 2006. *Rhythms of the Brain*. Oxford University Press.
- Buzsáki, G., Wang, X.J., 2012. Mechanisms of gamma oscillations. *Annu. Rev. Neurosci.* 35, 203–225.
- Campbell, A.E., Sumner, P., Singh, K.D., Muthukumaraswamy, S.D., 2014. Acute effects of alcohol on stimulus-induced gamma oscillations in human primary visual and motor cortices. *Neuropsychopharmacology* 39 (9), 2104–2113.
- Chaieb, L., Antal, A., Paulus, W., 2008. Gender-specific modulation of short-term neuroplasticity in the visual cortex induced by transcranial direct current stimulation. *Vis. Neurosci.* 25 (1), 77–81.
- Chatrjan, G.E., Lettich, E., Nelson, P.L., 1985. Ten percent electrode system for topographic studies of spontaneous and evoked EEG activity. *Am. J. EEG Technol.* 25, 83–92.
- Chen, R., Hallett, M., 1999. The time course of changes in motor cortex excitability associated with voluntary movement. *Can. J. Neurol. Sci.* 26 (3), 163–169.
- Chen, R., Yaseen, Z., Cohen, L.G., Hallett, M., 1998. Time course of corticospinal excitability in reaction time and self-paced movements. *Ann. Neurol.* 44 (3), 317–325.
- Cheyne, D.O., 2013. MEG studies of sensorimotor rhythms: a review. *Exp. Neurol.* 245, 27–39.
- Cheyne, D., Weinberg, H., 1989. Neuromagnetic fields accompanying unilateral finger movements: pre-movement and movement-evoked fields. *Exp. Brain Res.* 78 (3), 604–612.
- Clark, V.P., Coffman, B.A., Trumbo, M.C., Gasparovic, C., 2011. Transcranial direct current stimulation (tDCS) produces localized and specific alterations in neurochemistry: a 1 H magnetic resonance spectroscopy study. *Neurosci. Lett.* 500 (1), 67–71.
- Creutzfeldt, O.D., Fromm, G.H., Kapp, H., 1962. Influence of transcranial dc currents on cortical neuronal activity. *Exp. Neurol.* 5 (6), 436–452.
- Deecke, L., Weinberg, H., Brickett, P., 1982. Magnetic fields of the human brain accompanying voluntary movement: Bereitschaftsmagnetfeld. *Exp. Brain Res.* 48 (1), 144–148.
- Di Russo, F., Martínez, A., Sereno, M.I., Pitzalis, S., Hillyard, S.A., 2002. Cortical sources of the early components of the visual evoked potential. *Hum. Brain Mapp.* 15 (2), 95–111.
- Donner, T.H., Siegel, M., 2011. A framework for local cortical oscillation patterns. *Trends Cogn. Sci.* 15 (5), 191–199.
- Fregni, F., Boggio, P.S., Santos, M.C., Lima, M., Vieira, A.L., Rigonatti, S.P., Pascual-Leone, A., 2006. Noninvasive cortical stimulation with transcranial direct current stimulation in Parkinson's disease. *Mov. Disord.* 21 (10), 1693–1702.
- Fresnoza, S., Paulus, W., Nitsche, M.A., Kuo, M.F., 2014. Nonlinear dose-dependent impact of D1 receptor activation on motor cortex plasticity in humans. *J. Neurosci.* 34 (7), 2744–2753.

- Froc, D.J., Chapman, C.A., Trepel, C., Racine, R.J., 2000. Long-term depression and depotentiation in the sensorimotor cortex of the freely moving rat. *J. Neurosci.* 20 (1), 438–445.
- Gonzalez-Burgos, G., Lewis, D.A., 2008. GABA neurons and the mechanisms of network oscillations: implications for understanding cortical dysfunction in schizophrenia. *Schizophr. Bull.* 34 (5), 944–961.
- Hall, S.D., Barnes, G.R., Furlong, P.L., Seri, S., Hillebrand, A., 2010. Neuronal network pharmacodynamics of GABAergic modulation in the human cortex determined using pharmac-magnetoencephalography. *Hum. Brain Mapp.* 31 (4), 581–594.
- Hasenstaub, A., Shu, Y., Haider, B., Kraushaar, U., Duque, A., McCormick, D.A., 2005. Inhibitory postsynaptic potentials carry synchronized frequency information in active cortical networks. *Neuron* 47 (3), 423–435.
- Helfrich, R.F., Schneider, T.R., Rach, S., Trautmann-Lengsfeld, S.A., Engel, A.K., Herrmann, C.S., 2014. Entrainment of brain oscillations by transcranial alternating current stimulation. *Curr. Biol.* 24 (3), 333–339.
- Hipp, J.F., Engel, A.K., Siegel, M., 2011. Oscillatory synchronization in large-scale cortical networks predicts perception. *Neuron* 69 (2), 387–396.
- Horvath, J.C., Carter, O., Forte, J.D., 2014. Transcranial direct current stimulation: five important issues we aren't discussing (but probably should be). *Front. Syst. Neurosci.* 8. <http://dx.doi.org/10.3389/fnsys.2014.00002>.
- Horvath, J.C., Forte, J.D., Carter, O., 2015. Evidence that transcranial direct current stimulation (tDCS) generates little-to-no reliable neurophysiologic effect beyond MEP amplitude modulation in healthy human subjects: a systematic review. *Neuropsychologia* 66, 213–236.
- Huang, M.X., Mosher, J.C., Leahy, R.M., 1999. A sensor-weighted overlapping-sphere head model and exhaustive head model comparison for MEG. *Phys. Med. Biol.* 44, 423–440.
- Hunter, M.A., Coffman, B.A., Trumbo, M.C., Clark, V.P., 2013. Tracking the neuroplastic changes associated with transcranial direct current stimulation: a push for multimodal imaging. *Front. Hum. Neurosci.* 7. <http://dx.doi.org/10.3389/fnhum.2013.00495>.
- Jacobson, L., Ezra, A., Berger, U., Lavidor, M., 2012. Modulating oscillatory brain activity correlates of behavioral inhibition using transcranial direct current stimulation. *Clin. Neurophysiol.* 123 (5), 979–984.
- Jeffreys, D.A., Axford, J.G., 1972a. Source locations of pattern-specific components of human visual evoked potentials. I. Component of striate cortical origin. *Exp. Brain Res.* 16 (1), 1–21.
- Jeffreys, D.A., Axford, J.G., 1972b. Source locations of pattern-specific components of human visual evoked potentials. II. Components of extra-striate cortical origin. *Exp. Brain Res.* 16 (1), 22–40.
- Jensen, O., Pohja, M., Goel, P., Ermentrout, B., Kopell, N., Hari, R., 2002. On the physiological basis of the 15–30 Hz motor-cortex rhythm. *Proceedings of the 13th International Conference on Biomagnetism*. VDE Verlag GMBH, Berlin, pp. 313–315.
- Jensen, O., Goel, P., Kopell, N., Pohja, M., Hari, R., Ermentrout, B., 2005. On the human sensorimotor-cortex beta rhythm: sources and modeling. *Neuroimage* 26 (2), 347–355.
- Jurkiewicz, M.T., Gaetz, W.C., Bostan, A.C., Cheyne, D., 2006. Post-movement beta rebound is generated in motor cortex: evidence from neuromagnetic recordings. *Neuroimage* 32 (3), 1281–1289.
- Kristeva, R., Cheyne, D., Deecke, L., 1991. Neuromagnetic fields accompanying unilateral and bilateral voluntary movements: topography and analysis of cortical sources. *Electroencephalogr. Clin. Neurophysiol.* 81 (4), 284–298.
- Lang, N., Siebner, H.R., Chadaide, Z., Boros, K., Nitsche, M.A., Rothwell, J.C., Antal, A., 2007. Bidirectional modulation of primary visual cortex excitability: a combined tDCS and rTMS study. *Invest. Ophthalmol. Vis. Sci.* 48 (12), 5782–5787.
- Le Van Quyen, M., Foucher, J., Lachaux, J., Rodriguez, E., Lutz, A., Martinerie, J., Varela, F.J., 2001. Comparison of Hilbert transform and wavelet methods for the analysis of neuronal synchrony. *J. Neurosci. Methods* 111, 83–98.
- Leuthold, H., Jentsch, I., 2002. Distinguishing neural sources of movement preparation and execution: an electrophysiological analysis. *Biol. Psychol.* 60 (2), 173–198.
- Liebetanz, D., Nitsche, M.A., Tergau, F., Paulus, W., 2002. Pharmacological approach to the mechanisms of transcranial DC-stimulation-induced after-effects of human motor cortex excitability. *Brain* 125 (10), 2238–2247.
- Mahmoudi, H., Haghighi, A.B., Petramfar, P., Jahanshahi, S., Salehi, Z., Fregni, F., 2011. Transcranial direct current stimulation: electrode montage in stroke. *Disabil. Rehabil.* 33, 1383–1388.
- Mangia, A.L., Pirini, M., Cappello, A., 2014. Transcranial direct current stimulation and power spectral parameters: a tDCS/EEG co-registration study. *Front. Hum. Neurosci.* 8. <http://dx.doi.org/10.3389/fnhum.2014.00601>.
- Matsunaga, K., Nitsche, M.A., Tsuji, S., Rothwell, J.C., 2004. Effect of transcranial DC sensorimotor cortex stimulation on somatosensory evoked potentials in humans. *Clin. Neurophysiol.* 115 (2), 456–460.
- Monte-Silva, K., Kuo, M.F., Hesselthaler, S., Fresnoza, S., Liebetanz, D., Paulus, W., Nitsche, M.A., 2013. Induction of late LTP-like plasticity in the human motor cortex by repeated non-invasive brain stimulation. *Brain Stimul.* 6 (3), 424–432.
- Muthukumaraswamy, S.D., 2010. Functional properties of human primary motor cortex gamma oscillations. *J. Neurophysiol.* 104 (5), 2873–2885.
- Muthukumaraswamy, S.D., Singh, K.D., Swettenham, J.B., Jones, D.K., 2010. Visual gamma oscillations and evoked responses: variability, repeatability and structural MRI correlates. *Neuroimage* 49 (4), 3349–3357.
- Muthukumaraswamy, S.D., Myers, J.F.M., Wilson, S.J., Nutt, D.J., Lingford-Hughes, A., Singh, K.D., Hamandi, K., 2013a. The effects of elevated endogenous GABA levels on movement-related network oscillations. *NeuroImage* 66, 36–41.
- Muthukumaraswamy, S.D., Carhart-Harris, R.L., Moran, R.J., Brookes, M.J., Williams, T.M., Erritzoe, D., Nutt, D.J., 2013b. Broadband cortical desynchronization underlies the human psychedelic state. *J. Neurosci.* 33 (38), 15171–15183.
- Neuling, T., Rach, S., Wagner, S., Wolters, C.H., Herrmann, C.S., 2012. Good vibrations: oscillatory phase shapes perception. *Neuroimage* 63 (2), 771–778.
- Neuling, T., Ruhnau, P., Fuscà, M., Demarchi, G., Herrmann, C.S., Weisz, N., 2015. Friends, not foes: magnetoencephalography as a tool to uncover brain dynamics during transcranial alternating current stimulation. *NeuroImage* 118, 406–413.
- Nitsche, M.A., Paulus, W., 2000. Excitability changes induced in the human motor cortex by weak transcranial direct current stimulation. *J. Physiol.* 527 (3), 633–639.
- Nitsche, M.A., Paulus, W., 2001. Sustained excitability elevations induced by transcranial DC motor cortex stimulation in humans. *Neurology* 57, 1899–1901.
- Nitsche, M.A., Fricke, K., Henschke, U., Schlitterlau, A., Liebetanz, D., Lang, N., 2003. Pharmacological modulation of cortical excitability shifts induced by transcranial direct current stimulation in humans. *J. Physiol.* 553 (1), 293–301.
- Nitsche, M.A., Liebetanz, D., Schlitterlau, A., Henschke, U., Fricke, K., Frommann, K., Tergau, F., 2004. GABAergic modulation of DC stimulation-induced motor cortex excitability shifts in humans. *Eur. J. Neurosci.* 19 (10), 2720–2726.
- Notturmo, F., Marzetti, L., Pizzella, V., Uncini, A., Zappasodi, F., 2014. Local and remote effects of transcranial direct current stimulation on the electrical activity of the motor cortical network. *Hum. Brain Mapp.* 35 (5), 2220–2232.
- Oldfield, R.C., 1971. The assessment and analysis of handedness: the Edinburgh inventory. *Neuropsychologia* 9 (1), 97–113.
- Pelli, D.G., 1997. The VideoToolbox software for visual psychophysics: transforming numbers into movies. *Spat. Vis.* 10, 437–442.
- Pellicciari, M.C., Brignani, D., Miniussi, C., 2013. Excitability modulation of the motor system induced by transcranial direct current stimulation: a multimodal approach. *NeuroImage* 83, 569–580.
- Pfurtscheller, G., Lopes da Silva, F., 1999. Event-related EEG/MEG synchronization and desynchronization: basic principles. *Clin. Neurophysiol.* 110 (11), 1842–1857.
- Polanía, R., Nitsche, M.A., Paulus, W., 2011. Modulating functional connectivity patterns and topological functional organization of the human brain with transcranial direct current stimulation. *Hum. Brain Mapp.* 32 (8), 1236–1249.
- Polanía, R., Paulus, W., Nitsche, M.A., 2012. Modulating cortico-striatal and thalamo-cortical functional connectivity with transcranial direct current stimulation. *Hum. Brain Mapp.* 33 (10), 2499–2508.
- Purpura, D.P., McMurtry, J.G., 1965. Intracellular activities and evoked potential changes during polarization of motor cortex. *J. Neurophysiol.* 28 (1), 166–185.
- Reato, D., Rahman, A., Bikson, M., Parra, L.C., 2010. Low-intensity electrical stimulation affects network dynamics by modulating population rate and spike timing. *J. Neurosci.* 30 (45), 15067–15079.
- Reato, D., Bikson, M., Parra, L.C., 2014. Lasting modulation of in-vitro oscillatory activity with weak direct current stimulation. *J. Neurophysiol.* <http://dx.doi.org/10.1152/jn.00208.2014>.
- Robinson, S.E., Vrba, J., 1999. Recent advances in biomagnetism. *Functional Neuroimaging by Synthetic Aperture Magnetometry (SAM)*. Tohoku University Press Sendai, Japan, pp. 302–305.
- Rönnqvist, K.C., McAllister, C.J., Woodhall, G.L., Stanford, I.M., Hall, S.D., 2013. A multimodal perspective on the composition of cortical oscillations. *Front. Hum. Neurosci.* (7) <http://dx.doi.org/10.3389/fnhum.2013.00132>.
- Roy, A., Baxter, B., He, B., 2014. High definition transcranial direct current stimulation induces both acute and persistent changes in broadband cortical synchronization: a simultaneous tDCS–EEG study. *IEEE Trans. Biomed. Eng.* 61 (7), 1967–1978.
- Schutter, D.J., Hortensius, R., 2011. Brain oscillations and frequency-dependent modulation of cortical excitability. *Brain Stimul.* 4 (2), 97–103.
- Sehm, B., Kipping, J., Schäfer, A., Villringer, A., Ragert, P., 2013. A comparison between uni- and bilateral tDCS effects on functional connectivity of the human motor cortex. *Front. Hum. Neurosci.* 7. <http://dx.doi.org/10.3389/fnhum.2013.00183>.
- Shibasaki, H., Hallett, M., 2006. What is the Bereitschaftspotential? *Clin. Neurophysiol.* 117 (11), 2341–2356.
- Singer, W., Gray, C.M., 1995. Visual feature integration and the temporal correlation hypothesis. *Annu. Rev. Neurosci.* 18 (1), 555–586.
- Smith, S.M., 2002. Fast robust automated brain extraction. *Hum. Brain Mapp.* 17 (3), 143–155.
- Soekadar, S.R., Witkowski, M., Cossio, E.G., Birbaumer, N., Robinson, S.E., Cohen, L.G., 2013. In vivo assessment of human brain oscillations during application of transcranial electric currents. *Nat. Commun.* 4. <http://dx.doi.org/10.1038/ncomms3032>.
- Spitoni, G.F., Cimmino, R.L., Bozzacchi, C., Pizzamiglio, L., Di Russo, F., 2013. Modulation of spontaneous alpha brain rhythms using low-intensity transcranial direct-current stimulation. *Front. Hum. Neurosci.* 7. <http://dx.doi.org/10.3389/fnhum.2013.00529>.
- Stagg, C.J., Nitsche, M.A., 2011. Physiological basis of transcranial direct current stimulation. *Neuroscientist* 17 (1), 37–53.
- Stagg, C.J., Best, J.G., Stephenson, M.C., O'Shea, J., Wylezinska, M., Kincses, Z.T., Johansen-Berg, H., 2009. Polarity-sensitive modulation of cortical neurotransmitters by transcranial stimulation. *J. Neurosci.* 29 (16), 5202–5206.
- Swettenham, J.B., Muthukumaraswamy, S.D., Singh, K.D., 2009. Spectral properties of induced and evoked gamma oscillations in human early visual cortex to moving and stationary stimuli. *J. Neurophysiol.* 102 (2), 1241–1253.
- Tallon-Baudry, C., Bertrand, O., 1999. Oscillatory gamma activity in humans and its role in object representation. *Trends Cogn. Sci.* 3 (4), 151–162.
- Thut, G., Miniussi, C., Gross, J., 2012. The functional importance of rhythmic activity in the brain. *Curr. Biol.* 22 (16), 658–663.
- Venkatakrishnan, A., Contreras-Vidal, J.L., Sandrini, M., Cohen, L.G., 2011. Independent component analysis of resting brain activity reveals transient modulation of local cortical processing by transcranial direct current stimulation. *Engineering in Medicine*

- and Biology Society, EMBC, 2011 Annual International Conference of the IEEE, pp. 8102–8105.
- Vrba, J., Robinson, S.E., 2001. Signal processing in magnetoencephalography. *Methods* 25 (2), 249–271.
- Xia, M., Wang, J., He, Y., 2013. BrainNet viewer: a network visualization tool for human brain connectomics. *PLoS One* 8 (7). <http://dx.doi.org/10.1371/journal.pone.0068910>.
- Yamawaki, N., Stanford, I.M., Hall, S.D., Woodhall, G.L., 2008. Pharmacologically induced and stimulus evoked rhythmic neuronal oscillatory activity in the primary motor cortex in vitro. *Neuroscience* 151 (2), 386–395.
- Zaehle, T., Rach, S., Herrmann, C.S., 2010. Transcranial alternating current stimulation enhances individual alpha activity in human EEG. *PLoS One* 5 (11). <http://dx.doi.org/10.1371/journal.pone.0013766>.